Design and Cyclic Elastoplastic Analysis of Graded Thin-Walled Steel Tubular Columns with Enhanced Strength and Ductility

Qusay Al-Kaseasbeh
University of North Dakota
qusay.alkaseasbeh@ndus.edu

Iraj H. P. Mamaghani
University of North Dakota
iraj.mamaghani@engr.und.edu

Abstract

Thin-walled steel stiffened box columns are widely used as cantilever bridge piers due to their structural efficiency, attractive appearance, high earthquake resistance, and potential for concrete infilling. However, local buckling, global buckling, or combination of both is usually the main reason of significant strength reduction in these columns, which eventually leads to their collapse. This paper investigates the behavior of thin-walled steel stiffened box column with uniform (B), and graded thickness (GB) under constant axial and cyclic lateral loading. A GB column with size and volume of material equivalent to uniform B column is introduced and analyzed under constant axial and cyclic lateral loading. The analysis is carried out using a finite-element model (FEM), which considers both material and geometric nonlinearities. The accuracy of the employed FEM is validated based on the experimental results available in the literature. The GB column shows a superior strength and ductility performance. An improvement of 24% in the ultimate strength is achieved using the GB column as compared to its counterpart B column. The buckling behavior of the B column is captured relatively well by the FEM. The local buckling behavior is delayed and less severe in the case of the GB column as compared to its counterpart B column. Moreover, the dissipated energy of the GB column is higher, which exhibited higher ductility than that of the B column. Finally, the cyclic behavior of the B column is greatly improved with longitudinal stiffeners.

Introduction

In severe seismic regions, civil engineering structures are exposed to increased earthquake risk. Their integrity is always threatened due to extreme uncertainties of severe earthquakes (Miller, 1998; Mahin, 1998; Nakashima, Inoue, & Tada,1998; Al-Kaseasbeh, Lin, Wang, Azarmi, & Qi, 2018; Al-Kaseasbeh, 2015). Thin-walled steel stiffened box columns are widely used in modern buildings, offshore platforms, elevated storage tanks, transmission towers, and wind turbines. Additionally, they can be used as cantilever bridge piers in seismic regions due to their structural efficiency, aesthetic attractive appearance, high earthquake resistance, and potential for concrete infilling (Ucak & Tsopelas, 2014). Compared to their counterparts of reinforced concrete, thin-walled steel stiffened box columns are more efficient due to their light weight, high strength, ductility, and ease and

speed of construction, especially when limited construction space is available (Yang, Zhao, Sun, & Zhao, 2017; Mamaghani, 1996). Thin-walled steel stiffened box columns are susceptible to a significant loss of strength and ductility under severe earthquakes; e.g., the 1995 Kobe earthquake, the 2008 Sichuan earthquake, and the 2011 East Japan earthquake (Ucak & Tsopelas, 2014). Thin-walled steel stiffened box columns experienced excessive local buckling and then collapse due to severe earthquakes (Bruneau, 1998). As a result, conventional uniform thin-walled steel stiffened box columns have been extensively investigated in the past few decades.

Many experimental and numerical analyses have been conducted to improve the strength and ductile behavior of the thin-walled steel stiffened box columns under axial and cyclic lateral loading (Yang et al., 2017; Ucak & Tsopelas, 2014). A numerical study has been conducted to investigate factors that affect strength and ductility capacities of unstiffened box sections (Usami & Ge, 1998). The ultimate strength of thin-walled steel stiffened box columns depends on the width-to-thickness ratio parameter, R_f, and the slenderness ratio parameter, λ (Kwon, Kim, & Hancock, 2007). In general, local buckling is affected by R_f of the column, while λ controls the global buckling of the column (Bruneau, 1998; Fukumoto, 2004; Usami, & Ge, 1998). An experimental and analytical investigation on the effectiveness of retrofitting the stiffened box cross sections was carried out by different researchers (Kwon, Kim, & Hancock, 2007; Goto, Wang, & Obata, 1998; Mamaghani, 2008). The study concluded that all retrofit schemes including: diaphragms, longitudinal stiffeners, corner reinforcement, inner cruciform plates, corner plates, and concrete infill improves the column's strength and ductility (Susantha, Aoki, Kumano, & Yamamoto, 2005). Setting diaphragms in short distances along the column height delays the local buckling occurrence (Ge, Gao, & Usami, 2000). New thin-walled corrugated and cellular steel columns demonstrate superior performance in strength, ductility, and post-buckling behavior under constant axial and cyclic lateral loading (Ucak & Tsopelas, 2014). Columns with tapered plates improved the ultimate strength and ductility of steel bridge piers (Mamaghani & Packer, 2002; Mamaghani, 2005).

This study numerically studied a tested uniform thin-walled steel stiffened box column (B) under constant axial and cyclic lateral loading. The comparison between the obtained results from FE analysis and the experiment, confirms the validity of FE analysis, and a GB column with size and volume of material equivalent to a B column is proposed to improve the strength, ductility, and post-buckling behavior of B columns. The results indicate that an improvement of 24% in the ultimate strength is achieved using the GB columns. The GB column delays the local buckling occurrence. Moreover, local buckling is less severe in the case of the GB column as compared to its counterpart B column. The dissipated energy of the graded-thickness steel tubular columns is higher which exhibited higher ductility. The main reason for the improved behavior of GB columns is the ability of these columns to eliminate the severity of local buckling near the column base, where the buckling usually occurs.

Finite Element Analysis

There is no doubt that full-scale testing results in a better insight into understanding the structures' behavior; however, physical experimentation is expensive, and time consuming. For this purpose, finite element analysis is conducted on the thin-walled steel stiffened box

columns cyclic behavior using ABAQUS software (Hibbit, Karlsson, & Sorensen, 2014). The FEM takes into account both material and geometric nonlinearities. The key design parameters considered in the practical design of thin-walled steel box columns are R_f, and λ (Mamaghani & Packer, 2002). R_f is concerned with the local buckling behavior of thin-walled steel box columns, while λ controls the global buckling (Fukumoto, 2004; Usami & Ge, 1998). These parameters are defined as follows:

$$R_f = \frac{b}{t}\frac{1}{n\pi}\sqrt{3\left(1-\nu^2\right)\frac{\sigma_y}{E}} \tag{1}$$

$$\lambda = \frac{2h}{r}\frac{1}{\pi}\sqrt{\frac{\sigma_y}{E}} \tag{2}$$

Where h = column height; r = radius of gyration; σ_y = yield stress; E = Young's modulus; v = Poisson's ratio; b = Cross-section width; n = number of subpanels of each plate; and t = plate thickness.

Under constant axial and cyclic lateral loading, local buckling usually occurs near the column's base (Nishikawa et al., 1998). For this purpose, beam element, B31, is employed for the upper part of the column (h-2b), whereas four-node shell element with reduced integration, S4R, is used for the lower part of the column (2b), as shown in Figure 1. S4R elements are able to accurately model the local buckling effect. All used elements are available in the ABAQUS library (Hibbit, Karlsson, & Sorensen, 2014). The interface between S4R and B31 elements is modeled using multi-point constraint (MPC). The column is fixed at its base and subjected to a constant axial load (P) and cyclic lateral displacement at the top. For computational efficiency, the bottom half of the lower part (b) is divided into 26 S4R elements, while the remaining height (b) is only divided into 14 S4R elements. The upper part of the column (height of h-2b) is divided into 14 elements. The mesh divisions presented above are determined by trial-and-error. Such mesh sizes give accurate results without increasing the computational time. The initial geometrical imperfection and residual stresses are not accounted in the FE analysis as their effect was not measured for the tested column (Nishikawa et al.,1998). Moreover, both initial geometrical imperfection and residual stresses have insignificant influence on the overall cyclic behavior after the first half-cycle (Ge, Gao, & Usami, 2000; Takaku, Fukumoto, & Aoki, 2004; Hibbit, Karlsson, & Sorensen, 2014). Table 1 lists the geometrical properties of the analyzed columns.

Cyclic Loading Program

The displacement-controlled unidirectional cyclic loading is adopted as a lateral loading program and illustrated in Figure 1d. At the top of the column, a combination of quasi-static cyclic lateral loading and constant axial load (P) is applied throughout the loading history. The displacement amplitude of the cyclic displacement is increased as a multiple of the yield displacement (δ_y), which is defined by Equation 3:

$$\delta_y = \frac{H_y h^3}{3E_s I_s} \tag{3}$$

Where $H_y = (\sigma_y - P/A)\, Z/h$ = lateral yield load and A, h, EI, and Z = cross-sectional area, the height, the bending stiffness, and the section modulus, respectively, of the B column (Goto, Kumar, & Kawanishi, 2010). The lateral yield load and yield displacement of the tested column are listed in Table 1. All the analyzed columns are assumed to be made of carbon steel SS400 (JIS, 2012), equivalent to ASTM A36 (ASTM, 2014)

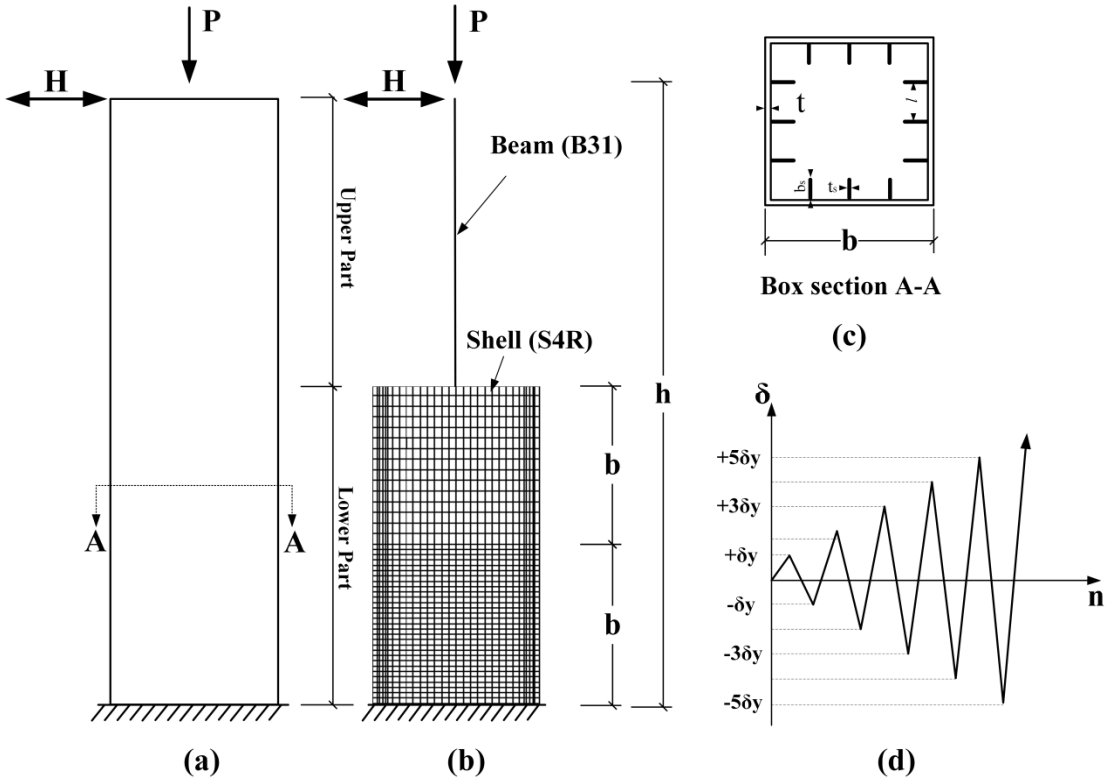

Figure 1. B Column model: (a) column; (b) FE meshing; (c) cross section; and (d) loading program.

Thin-Walled Steel Stiffened Box Column with Graded Thickness

Uniform B columns suffer premature buckling behavior (local buckling, global buckling, or a combination of both), near the column base, under constant axial and cyclic lateral loading (see Figure 1). This buckling behavior makes these columns unable to utilize their full strength and ductility. To overcome these shortcomings, graded-thickness stiffened box columns (GB) are used as alternatives for the counterpart conventional uniform B columns. The column height and width are kept same for both B and GB columns. The GB column is divided into three segments of constant cross sections. The first and second segments have the same height that is equal to the width (b) of the box section from the base. The third segment has a height of (h-2b). As shown in Figure 2, a thicker cross section (t_1=1.25t) is used along the first segment, and the original thickness (t_2= t) is kept for the second segment. Finally, the remaining material volume is distributed on the third segment with (t_3=0.86t). The above configurations of graded-thickness sections are chosen based on which achieved

better behavior. Table 1 shows material and geometrical properties of the B and GB columns. As seen in Table 1, same material and geometrical properties (except for the plate thickness) are used for both B and GB columns.

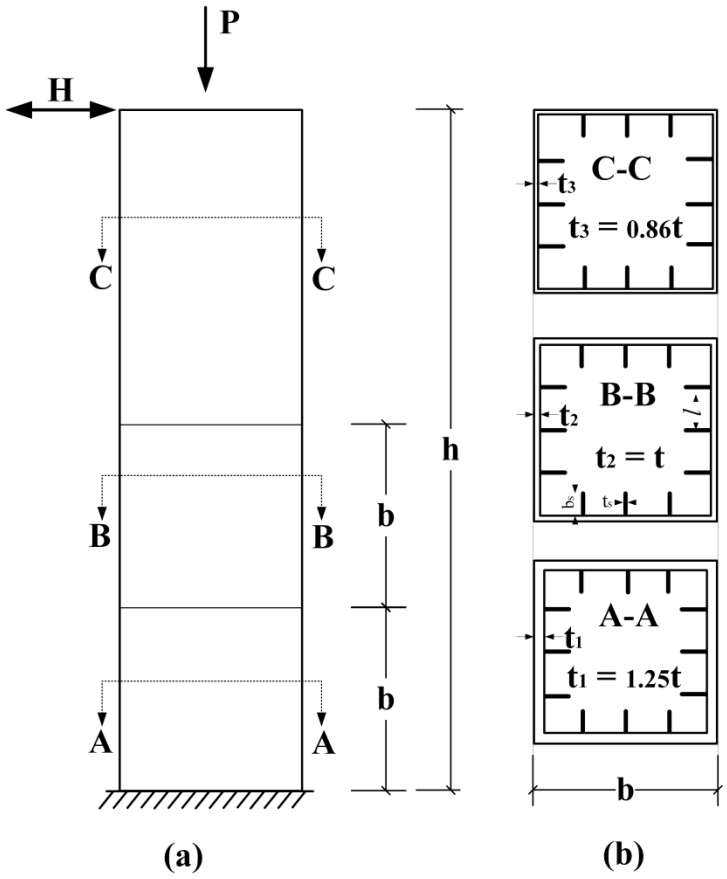

Figure 2. GB Column model: (a) column, and (b) graded-thickness sections.

Comparison of Numerical and Experimental Results

In this section, the numerical results of thin-walled steel stiffened box columns cyclic behavior are compared to the experimental results that were obtained by the Public Works Research Institute (PWRI) of Japan (Nishikawa et al., 1998).

Hysteresis Curves of B Columns

The normalized lateral load vs. lateral displacement hysteresis curves of B column obtained from the FE analysis and experiment, are shown in Figure 3a. In this figure, H_y and δ_y denote the lateral yield load and yield displacement, respectively. The comparison of hysteresis curves of B column shows a reasonable agreement with the experimental results. This indicates that FE analysis, using kinematic hardening material behavior, gives a reasonable accuracy to describe the material behavior with regard of local buckling of thin-walled steel stiffened box columns. At the end of the FE analysis, the buckling shape of B column (Figure 4b) is compared to the experimental buckling shape (Figure 4a) (Nishikawa et al., 1998). In

the experiment, the flange suffered from inward local buckling while the web buckled outward above the base of the column. The buckling shape is predicted relatively well by the adopted FEM. However, the outward buckling of the web in the analysis is not as prominent as in the experiment.

Table 1. Geometrical and material properties of the B column.

Properties	B Column*	GB Column
Steel Material	SM490	SM490
h (mm)	3403	3403
b (mm)	900	900
$t_1/t_2/t_3$ *(mm)*	9	11.25/ 9/ 7.75
b_s/t_s *(mm)*	80/6	80/6
(ns +1) x *l*	4×225	4×225
λ	0.26	0.26
R_f	0.56	0.56
H_y *(KN)*	1039	1039
δ_y *(mm)*	13.8	13.8
$P/\sigma_y A_s$	0.122	0.122
σ_y *(MPa)*	378.6	378.6
σ_u *(MPa)*	630	630
E (GPa)	206	206
v	0.3	0.3

*Reported in (Nishikawa et al., 1998).

Effect of Longitudinal Stiffeners on B Column Behavior

Figure 5 compares the effect of the longitudinal stiffeners on the lateral load and lateral displacement of the analyzed B columns with and without longitudinal stiffeners. The results indicate that cyclic behavior of the B column is greatly enhanced with the longitudinal stiffeners. For example, the normalized lateral vs. lateral displacement of the B column with longitudinal stiffeners is $H_m/H_y = 1.41$, while the $H_m/H_y = 0.65$ for the B column without the longitudinal stiffeners. As shown in Figure 4, the local buckling is more severe for the B column without longitudinal stiffeners (Figure 4d) as compared to the B column with longitudinal stiffeners (Figure 4b). Obviously, the longitudinal stiffeners prevent severe local buckling of the B column

Hysteresis Curves of B and GB Columns

Based on the Figure 3a, the compared FE analysis and experimental results indicate that the FEM is able to predict the nonlinear structural behavior with a reasonable accuracy. Using the validated FEM, a comparison study has been performed between the behavior of the B and GB columns under the same loading conditions. Figure 3b compares the hysteretic behavior of B and GB columns obtained from the FE analysis. The normalized ultimate strength (H_{max}/H_y) and normalized maximum displacement (δ_m/δ_y) of GB column are greater

than the B column by 24% and 32%, respectively. In the case of the B column, the buckling starts when the displacement is between $2\delta_y$ and $3\delta_y$. A drop of 36% of the ultimate strength (i.e. $H_{max}/H_y = 1.33$ observed at $\delta = +2.28\delta_y$) occurs at $\delta = +4\delta_y$. As the displacement increases, the column strength decreases at a fast rate to 14% of its maximum strength by the end of the analysis. By contrast, the GB column shows its H_{max}/H_y at $\delta = +3\delta_y$, which indicates that the local buckling occurs between $3\delta_y$ and $4\delta_y$. Only a 9% drop of the H_{max}/H_y takes place at $\delta = +4\delta_y$, while the residual strength of the GB column is 25% of its H_{max}/H_y at $\delta = +8\delta_y$. This comparison shows the superiority of the GB column and delay of local buckling occurrence in the GB column as compared to the B column. The final buckling shape of the GB column (Figure 4c) compared to the B column (Figure 4b) at the end of the analysis. The comparison shows that buckling is less severe in the case of the GB column as compared to its counterpart B column. The main reason for the improved behavior of GB columns is their ability to eliminate severe local buckling near the base of the column where the buckling usually occurs.

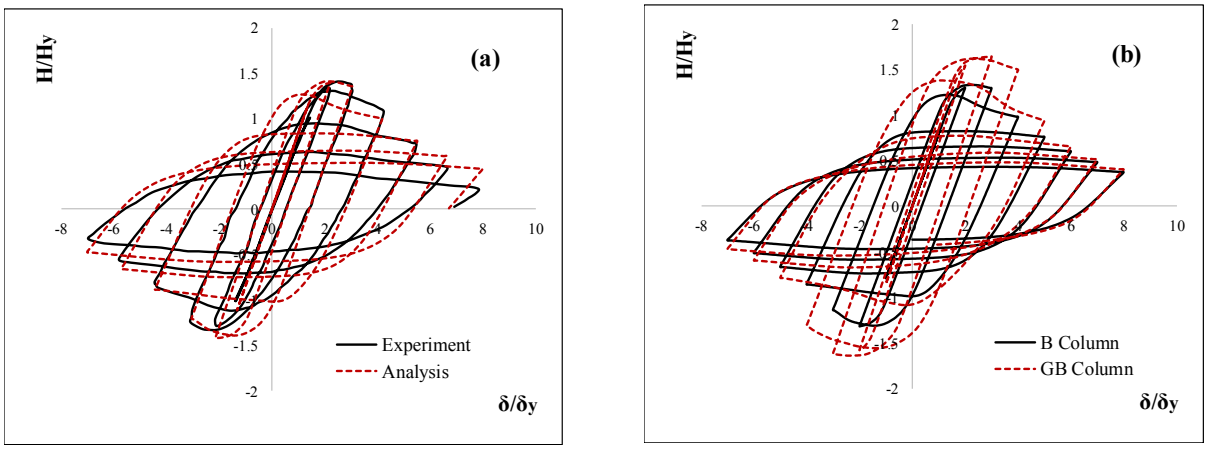

Figure 3. Comparison of lateral load vs. lateral displacement hysteresis curves.

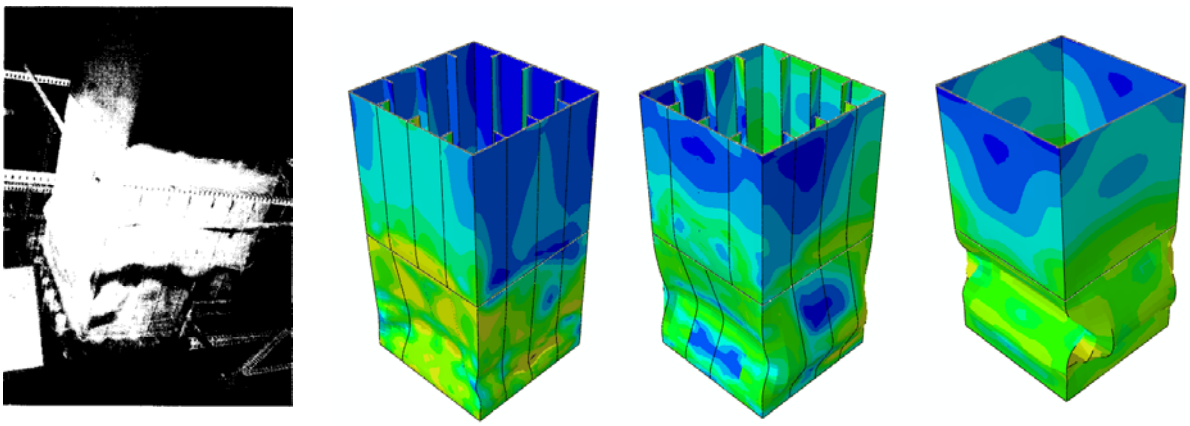

(a) **(b)** **(c)** **(d)**

Figure 4. Buckling shapes of columns: (a) experiment*, (b) B column with stiffeners, (c) GB column, and (d) B column without stiffeners. (*reported in Nishikawa et al., 1998)

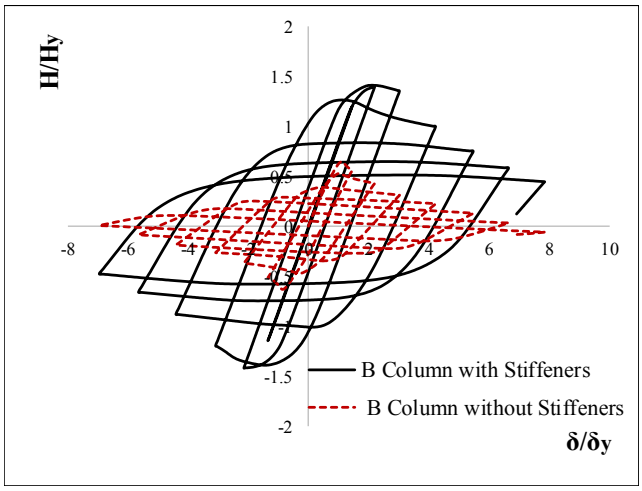

Figure 5. Effect of longitudinal stiffeners.

Energy Absorption Capacity

The dissipated energy is an objective indicator of the inelastic cyclic behavior of the structures. Accordingly, the energy absorption capacity of the column has been evaluated under cyclic behavior. A normalized energy absorption (E) is defined as follows (Mamaghani, Shen, Mizuno, & Usami, 1995):

$$E = \frac{I}{E_o} \sum_{i=1}^{n} E_i \tag{4}$$

$$E_o = \frac{I}{2} H_y \delta_y \tag{5}$$

In Equation 4, E_i = energy absorption in the i-th half-cycle, n = number of half-cycles (one half-cycle is defined from any zero-lateral load to the subsequent zero-lateral load). Figure 6a compares the normalized cumulative energy absorption vs. the number of half-cycles, obtained from the analysis and experiment of the B column. The normalized energy absorption curves vs. the number of half-cycles obtained from the analysis fit very close to the experimental results. For the GB column, as shown in Figure 3b, the strength of the GB columns decreases in a controlled rate from cycle to cycle compared to the B column, which is expected to dissipate larger energy than the B column under cyclic lateral loading. As an alternative method, the area under lateral load vs. lateral displacement curves is calculated. Figure 6b shows that the dissipated energy of the GB column is larger than the B column, which is expected to experience higher ductility in the case of the GB column.

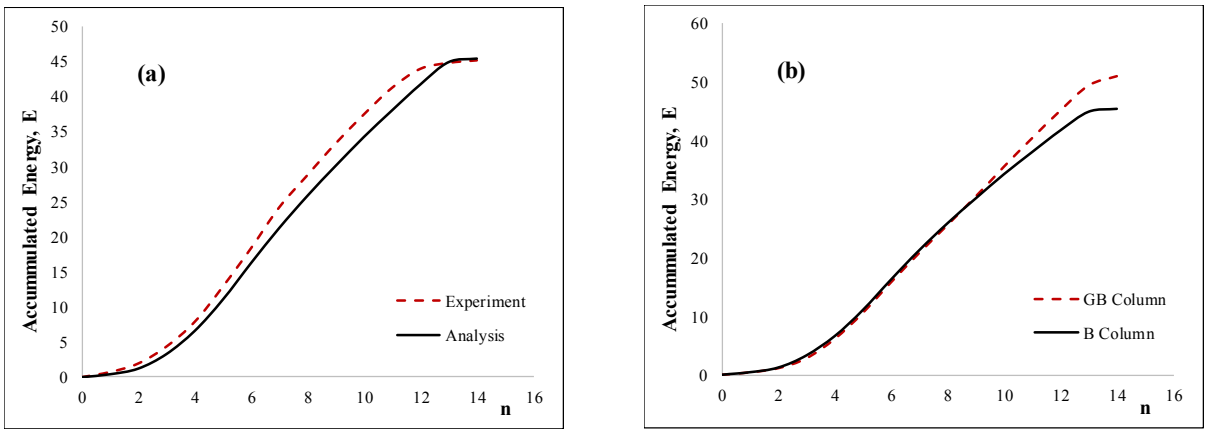

Figure 6. Energy absorption capacity.

Conclusions

This paper has described an FE analysis implementation to evaluate the cyclic behavior of the conventional B column of uniform cross section. In addition, a GB column with size and volume of material equivalent to a B column is introduced to improve the strength, ductility, and post-buckling behavior. First, the validity of the employed FEM was verified using the B column experimental results that are reported in the literature. The reasonable agreement between the FE analysis and experimental results confirms that the FEM can be used to capture the structural behavior with taking into account the local buckling behavior of thin-walled steel stiffened box columns. The GB column of graded section shows a superior strength and ductility performance. An improvement of 24% in the ultimate strength was achieved using the GB columns. Buckling behavior of the B columns was captured relatively well by the employed FEM. The GB column delays the local buckling occurrence, and local buckling is less severe in the case of the GB column as compared to its counterpart B column. Moreover, the dissipated energy of the GB columns was higher, which exhibited higher ductility. Finally, the cyclic behavior of the B column is greatly improved with the longitudinal stiffeners.

References

Al-Kaseasbeh, Q. (2015). *Electrochemical investigation of corrosion resistance of weldments in steel bridges*. Fargo, ND: North Dakota State University.

Al-Kaseasbeh, Q., Lin, Z., Wang, Y., Azarmi, F., & Qi, X. (2018). Electrochemical characterization of steel bridge welds under simulated durability test. *Journal of Bridge Engineering*, *23*(10). doi: 10.1061/(asce)be.1943-5592.0001246

ASTM. (2014). ASTM A36/A36M-14 standard specification for carbon structural steel. West Conshohocken, PA: ASTM International.

Bruneau, M. (1998). Performance of steel bridges during the 1995 Hyogoken–Nanbu (Kobe, Japan) earthquake—A North American perspective. *Engineering Structures*, *20*(12), 1063-1078.

Fukumoto, Y. (2004). Cyclic performance of stiffened square box columns with thickness

tapered plates. *Proceedings of the 2004 Annual Stability Conference*. Bethlehem, PA: SSRC.
Ge, H., Gao, S., & Usami, T. (2000). Stiffened steel box columns. Part 1: Cyclic behaviour. *Earthquake Engineering and Structural Dynamics*, *29*(11), 1691-1706.
Goto, Y., Wang, Q., & Obata, M. (1998). FEM Analysis for hysteretic behavior of thin-walled columns. *Journal of Structural Engineering*, *124*(11), 1290-1301.
Goto, Y., Kumar, G., & Kawanishi, N. (2010). Nonlinear finite-element analysis for hysteretic behavior of thin-walled circular steel columns with in-filled concrete. *Journal of Structural Engineering*, *136*(11), 1413-1422.
Hibbit, D., Karlsson, B., & Sorensen, P. (2014). *ABAQUS 2014 documentation*. Providence, RI: Dassault Systèmes.
JIS. (2012). *JIS handbook: Ferrous materials & metallurgy*. Tokyo, Japan: Japanese Standards Association.
Kwon, Y. B., Kim, N. G., & Hancock, G. J. (2007). Compression tests of welded section columns undergoing buckling interaction. *Journal of Constructional Steel Research*, *63*(12), 1590-1602.
Mahin, S. A. (1998). Lessons from damage to steel buildings during the Northridge earthquake. *Engineering Structures*, *20*(4-6), 261-270.
Mamaghani, I. H. P. (1996). *Cyclic elastoplastic behavior of steel structures: Theory and experiment*. Nagoya, Japan: Nagoya University.
Mamaghani, I. H. P. (2005). Assessment of earthquake resistance capacity and retrofit of steel tubular bridge piers. *Structural Engineers Association of California*, 357-370.
Mamaghani, I. H. P. (2008). Seismic design and ductility evaluation of thin-walled steel bridge piers of box sections. *Transportation Research Record: Journal of the Transportation Research Board*, *2050*(1), 137-142.
Mamaghani, I. H. P., & Packer, J. A. (2002). Inelastic behaviour of partially concrete-filled steel hollow sections. In *4th Structural Specialty Conference* (pp. 1–10). Montréal, Québec, Canada: Canadian Society for Civil Engineering.
Mamaghani, I. H. P., Usami, T., & Mizuno, E. (1996). Inelastic large deflection analysis of structural steel members under cyclic loading. *Engineering Structures*, *18*(9), 659-668.
Mamaghani, I. H. P., Shen, C., Mizuno, E., & Usami, T. (1995). Cyclic behavior of structural steels. I: Experiments. *Journal of Engineering Mechanics*, *121*(11), 1158-1164.
Miller, D. K. (1998). Lessons learned from the Northridge earthquake. *Engineering Structures*, *20*(4-6), 249-260.
Nakashima, M., Inoue, K., & Tada, M. (1998). Classification of damage to steel buildings observed in the 1995 Hyogoken-Nanbu earthquake. *Engineering Structures*, *20*(6), 271-281.
Nishikawa, K., Yamamoto, S., Natori, T., Terao, K., Yasunami, H., & Terada, M. (1998). Retrofitting for seismic upgrading of steel bridge columns. *Engineering Structures*, *20*(4-6), 540-551.
Susantha, K. A. S., Aoki, T., Kumano, T., & Yamamoto, K. (2005). Applicability of low-yield-strength steel for ductility improvement of steel bridge piers. *Engineering Structures*, *27*(7), 1064-1073.
Takaku, T., Fukumoto, Y., & Aoki, T. (2004). Seismic design of bridge piers with stiffened box sections using LP plates. *Proceedings of the 13th World Conference on Earthquake Engineering*. Tokyo, Japan: International Association for Earthquake

Engineering.
Ucak, A., & Tsopelas, P. (2014). Load path effects in circular steel columns under bidirectional lateral cyclic loading. *Journal of Structural Engineering*, *141*(5), 1-11.
Usami, T., & Ge, H. (1998). *Cyclic behavior of thin-walled steel structures—numerical analysis*. *Thin-walled structures* (vol. 32). Cambridge, MA: Elsevier.
Yang, C., Zhao, H., Sun, Y., & Zhao, S. (2017). Compressive stress-strain model of cold-formed circular hollow section stub columns considering local buckling. *Thin-Walled Structures*, *120*, 495-505.

Biographies

QUSAY AL-KASEASBEH is currently a PhD student of Civil Engineering at University of North Dakota. He earned his BSc in Civil Engineering from Mutah University, Jordan, in 2013 and an MSc in Civil Engineering from North Dakota State University in 2016. His main research interests are cyclic plasticity modeling of structural steel, advanced numerical analysis, stability and ductility evaluation of thin-walled steel structures, and seismic design of steel structures. Mr. Al-Kaseasbeh is available at qusay.alkaseasbeh@ndus.edu.

IRAJ H. P. MAMAGHANI is an associate professor of Civil Engineering at University of North Dakota. He works in the area of civil engineering, with emphasis on structural mechanics and structural engineering. He focuses on cyclic elastoplastic material modeling, structural stability, seismic design, advanced finite element analysis, and ductility evaluation of steel structures. Contact Dr. Mamaghani at iraj.mamaghani@engr.und.edu.

References

[1] Miller, D. K. (1998). Lessons learned from the Northridge earthquake. *Engineering Structures*, *20*(4–6), 249–260.

[2] Mahin, S. A. (1998). Lessons from damage to steel buildings during the Northridge earthquake. *Engineering Structures*, *20*(4–6), 261–270.

[3] Nakashima, M., Inoue, K., & Tada, M. (1998). Classification of damage to steel buildings observed in the 1995 Hyogoken-Nanbu earthquake. *Engineering Structures*, *20*(6), 271–281.

[4] Al-Kaseasbeh, Q., Lin, Z., Wang, Y., Azarmi, F., & Qi, X. (2018). Electrochemical Characterization of Steel Bridge Welds under Simulated Durability Test. *Journal of Bridge Engineering*, *23*(10), 4018068.

[5] Al-Kaseasbeh, Q. (2015). *Electrochemical Investigation of Corrosion Resistance of Weldments in Steel Bridges*. North Dakota State University.

[6] Ucak, A., & Tsopelas, P. (2014). Load Path Effects in Circular Steel Columns under Bidirectional Lateral Cyclic Loading. *Journal of Structural Engineering*, *141*, 1–11.

[7] Yang, C., Zhao, H., Sun, Y., & Zhao, S. (2017). Compressive stress-strain model of cold-formed circular hollow section stub columns considering local buckling. *Thin-Walled Structures*, *120*, 495–505.

[8] Mamaghani, I. H. P. (1996). *Cyclic Elastoplastic Behavior of steel structures: Theory and Experiment*. Nagoya University.

[9] Bruneau, M. (1998). Performance of steel bridges during the 1995 Hyogoken–Nanbu (Kobe, Japan) earthquake—a North American perspective. *Engineering Structures*, *20*(12), 1063–1078.

[10] Fukumoto, Y. (2004). Cyclic Performance of Stiffened Square Box Columns with Thickness Tapered Plates. In *Proceedings of the 2004 Annual Stability Conference, SSRC* (pp. 1–18).

[11] Usami, T., & Ge, H. (1998). *Cyclic behavior of thin-walled steel structures—numerical analysis*. *Thin-Walled Structures* (Vol. 32). Elsevier.

[12] Kwon, Y. B., Kim, N. G., & Hancock, G. J. (2007). Compression tests of welded section columns undergoing buckling interaction. *Journal of Constructional Steel Research*, *63*(12), 1590–1602.

[13] Goto, Wang, Q., & Obata, M. (1998). FEM Analysis for Hysteretic Behavior of Thin-Walled Columns. *Journal of Structural Engineering*, *124*(11), 1290–1301.

[14] Mamaghani, I. H. P. (2008). Seismic Design and Ductility Evaluation of Thin-Walled Steel Bridge Piers of Box Sections. *Transportation Research Record: Journal of the Transportation Research Board*, *2050*(1), 137–142.

[15] Mamaghani, I. H. P., & Packer, J. A. (2002). Inelastic behaviour of partially concrete-filled steel hollow sections. In *4th Structural Specialty Conference* (pp. 1–10).

[16] Mamaghani, I. H. P. (2004). Seismic design and retrofit of thin-walled steel tubular columns. In *13th World Conference on Earthquake Engineering*.

[17] Mamaghani, I. H. P. (2005). Assessment of Earthquake Resistance Capacity and Retrofit of Steel Tubular Bridge Piers. *Structural Engineers Association of California (SEAOC)*, 357–370.

[18] Nishikawa, K., Yamamoto, S., Natori, T., Terao, K., Yasunami, H., & Terada, M. (1998). Retrofitting for seismic upgrading of steel bridge columns. *Engineering*

Structures, *20*(4–6), 540–551.
[19] Susantha, K. A. S., Aoki, T., Kumano, T., & Yamamoto, K. (2005). Applicability of low-yield-strength steel for ductility improvement of steel bridge piers. *Engineering Structures*, *27*(7), 1064–1073.
[20] Ge, H., Gao, S., & Usami, T. (2000). Stiffened steel box columns. Part 1: Cyclic behaviour. *Earthquake Engineering and Structural Dynamics*, *29*(11), 1691–1706.
[21] Takaku, T., Fukumoto, Y., & Aoki, T. (2004). Seismic design of bridge piers with stiffened box sections using LP plates. In *iProceeding of the thirteenth world conference on earthquake engineering (on CD)*.
[22] Hibbit, Karlsson, & Sorensen. (2014). ABAQUS 2014 Documnetation. Dassault Systèmes, Providence, RI, USA.
[23] Hibbit, Karlsson, & Sorensen. (2014). Abaqus 2014 Documentation. Dassault.
[24] Banno, S., Mamaghani, I. H. P., Usami, T., & Mizuno, E. (1998). Cyclic Elastoplastic Large Deflection Analysis of Thin Steel Plates. *Journal of Engineering Mechanics*, *124*(4), 363–370.
[25] Mamaghani, I. H. P., Usami, T., & Mizuno, E. (1996). Cyclic elastoplastic large displacement behaviour of steel compression members. *Journal Of Structural Engineering*, *42*, 135–145.
[26] Goto, Y., Kumar, G., & Kawanishi, N. (2010). Nonlinear Finite-Element Analysis for Hysteretic Behavior of Thin-Walled Circular Steel Columns with In-Filled Concrete. *Journal of Structural Engineering*, *136*(11), 1413–1422.
[27] JIS. (2012). *JIS handbook: Ferrous Materials & Metallurgy*. Japanese Standards Association.
[28] ASTM. (2014). ASTM A36 / A36M - 14 Standard Specification for Carbon Structural Steel. *ASTM International, West Conshohocken, PA*, 12–14.
[29] Mamaghani, I. H. P., Shen, C., Mizuno, E., & Usami, T. (1995). Cyclic Behavior of Structural Steels. I: Experiments. *Journal of Engineering Mechanics*, *121*(11), 1158–1164.

Biographies

Qusay Al-Kaseasbeh is currently a PhD candidate of Civil Engineering at University of North Dakota (UND), USA. He earned his B.Sc. in Civil Engineering from Mutah University, Jordan, in 2013; and an MSc in Civil Engineering from North Dakota State University (NDSU), USA, in 2016. His main research interests are cyclic plasticity modeling of structural steel, advanced numerical analysis, stability and ductility evaluation of thin-walled steel structures, and seismic design of steel structures qusay.alkaseasbeh@ndus.edu.

Iraj H.P. Mamaghani is an Associate Professor of Civil Engineering at University of North Dakota (UND). He works in the area of civil engineering, with emphasis on structural mechanics and structural engineering. He focuses on cyclic elastoplastic material modeling, structural stability, seismic design, advanced finite element analysis and ductility evaluation of steel structures iraj.mamaghani@engr.und.edu.